Nano-architectured $Co(OH)_2$ electrodes constructed using an easily-manipulated electrochemical protocol for high-performance energy storage applications†

Jeng-Kuei Chang,*[a] Chih-Ming Wu[b] and I-Wen Sun*[b]

Received 1st December 2009, Accepted 15th February 2010
First published as an Advance Article on the web 9th March 2010
DOI: 10.1039/b925176f

A simple, low-cost, and efficient electrochemical strategy, which includes the co-deposition of a Ni–Cu layer, selective etching of Cu from the film (leaving nano-porous Ni), and electrodeposition of $Co(OH)_2$ nano-whiskers on the obtained Ni substrate, is used to construct a nano-structured electrode. This process can be conducted on many conductive surfaces, which can be cheap, flexible, and wearable, and can be integrated into advanced mobile micro-power systems. Due to its unique nano-architecture, the prepared $Co(OH)_2$ electrode shows exceptional energy storage performance as compared to that of the conventional version of the electrode. The optimum specific capacitance obtained in this study, evaluated using cyclic voltammetry (CV), was as high as 2800 F/g. When the CV scan rate was increased from 5 to 200 mV/s, only a 4% decay in the capacitance was found, indicating excellent high-power capability. These characteristics make the nano-structured $Co(OH)_2$ electrode a promising candidate for supercapacitor applications.

1. Introduction

In recent years, environmental issues and the depletion of fossil fuels have led to the accelerated development of alternative high-efficiency and clean energy conversion/storage systems that can meet present day power demands. Supercapacitors have a greater power density and a longer cycle life than those of batteries, and a higher energy density than that of conventional capacitors;[1,2] therefore, they have became increasingly attractive for use in hybrid electric vehicles, consumer electronics, medical devices, and military missile systems. Pseudocapacitors, whose capacitance is mainly attributed to the continuous and reversible redox reaction of electrode materials,[3,4] are one kind of supercapacitor. RuO_2 is a well-known material with ideal pseudocapacitive performance[5] and a specific capacitance of over 1000 F/g;[6,7] however, high cost substantially limits its commercial usage. $Co(OH)_2$ has recently received increasing attention because of its low cost, high redox activity, and great reversibility.[8–10] Some reported specific capacitances of $Co(OH)_2$[11,12] are even higher than that of RuO_2. Among the other alternatives to RuO_2 (*e.g.* MnO_x, CoO_x, NiO_x, and FeO_x), $Co(OH)_2$ shows a superior charge storage capability. Despite its importance, research on the pseudocapacitive properties of $Co(OH)_2$ has been limited. Further studies are required.

Nano-materials with a feature size ranging from a few to hundreds of nano-meters have great potential for electrochemical energy storage applications.[2,13] In a nano-structured electrode, the distance within the material over which electrolyte ions must be transported is shorter than that within a bulk electrode; furthermore, a large surface area allows for a high current density (or reaction rate) during the redox transition. As a result, a superior charge storage/delivery performance can be obtained as compared to that of a conventional bulk electrode.[14,15] It should be noted that nano-structures also lead to a high utilization of materials, resulting in a saving of natural resources and a lower electrode material cost. Construction of nano-architectured electrodes for supercapacitor applications has been attempted.[6,11,16,17] Self-supported oxide nanotubes or nanorods[7,18,19] and carbon- (*e.g.* CNTs or activated carbon) supported oxide nano-particles[20–22] have been fabricated to meet high power requirements. However, three major difficulties have been encountered: (i) nano-sized materials tend to re-agglomerate into large clusters (to lower the free energy), which decrease the porosity and surface area, (ii) the mechanical strength of electrodes with convex-architectures is usually unsatisfactory (*i.e.* they easily collapse or fall off), and (iii) the manufacturing cost of sophisticated nano-structures is relatively high. These issues should be dealt with before the proposed electrodes can be used in practice. Besides the miniaturization of the oxides/hydroxides, using nano-featured frameworks as substrates (or current collectors) for loading the electro-active materials is another approach to obtain nano-structured electrodes. Stainless steel mesh[23] and Ni foam substrates[24,25] have been found to improve the pseudocapacitive performance of electrodes; however, their pore sizes are on the micro-meter scale. A better electrode substrate with desirable nano-sized features is required.

Nano-porous Ni, developed from the selective dissolution of Cu from an electrodeposited Ni–Cu film, was examined in Searson's and our previous papers.[26–28] Recently, we have studied

[a]*Institute of Materials Science and Engineering, National Central University, 300 Jhongda Road, Taoyuan County, Taiwan. E-mail: catalyst@mail.mse.ncku.edu.tw*
[b]*Department of Chemistry, National Cheng Kung University, 1 University Road, Tainan City, Taiwan. E-mail: iwsun@mail.ncku.edu.tw*

† Electronic supplementary information (ESI) available: Cyclic voltammograms and chronopotentiogram of materials and the nano-structured $Co(OH)_2$ electrode. See DOI: 10.1039/b925176f

the possibility of using this kind of substrate to load MnO_2 and Co_3O_4 for energy storage applications.[29,30] In the present study, $Co(OH)_2$ is deposited on the porous Ni to construct a nano-architectured pseudocapacitive electrode. A much better pseudocapacitance, high-rate capability, and cyclic stability of the $Co(OH)_2$ electrode are demonstrated (as compared to those of MnO_2 and Co_3O_4). Moreover, the detailed formation characteristics of the Ni pores and the effects of thickness of the porous layer on the pseudocapacitive performance are investigated for the first time in this paper. It should be noted that the preparation of the nano-structured $Co(OH)_2$ electrode is an entirely electrochemical process, which has the advantages of simplicity, reliability, accuracy, versatility, and low-cost.[31,32] The nano-structure is also self-supported and binder-less. In general, the proposed protocol can be performed on any conductive surfaces, which can be inexpensive, lightweight, flexible, and wearable, that enables the prepared supercapacitors to be integrated into mobile micro-power systems. Another distinguishing feature of the proposed nano-porous substrate is the concave geometry (in contrast to the convex nanotubes and nanorods), which helps confine the active material within the pores and thus suppress collapse and aggregation.

2. Experimental

Ni–Cu alloy films were electrodeposited from a plating solution containing 1 M $NiSO_4$, 0.01 M $CuSO_4$, and 0.5 M H_3BO_3 (pH = 4). The deposition process was performed at 25 °C in a three-electrode cell with a platinum counter electrode and a saturated calomel reference electrode (SCE). Ni foil with an exposed area of 1 cm^2 was used as the working electrode. The films were deposited under a constant potential of −0.75 V, and the total cathodic passed charge was controlled to be 1, 2, 3, and 4 C/cm^2, respectively. Selective dissolution of Cu from the deposited Ni–Cu films with various thicknesses was then conducted in the same solution by applying an anodic potential of 0.2 V; the developed nano-porous Ni electrodes are denoted as Ni-1C, Ni-2C, Ni-3C, and Ni-4C, respectively. Surface morphologies and elemental compositions of the samples were examined using a scanning electron microscope (SEM, Philip XL-40 FEG) and its auxiliary X-ray energy dispersive spectroscope (EDS). X-ray photoelectron spectroscopy (XPS) was employed to study the chemical states of the film before and after the selective dissolution; the analyses were performed with a PHI 5000 Versa-Probe spectrometer utilizing monochromated Al Kα radiation as the X-ray source.

$Co(OH)_2$ was electrodeposited onto the prepared nano-porous Ni substrates and a flat Ni foil (as a counterpart) in 0.1 M $Co(CH_3COO)_2$ aqueous solution at 25 °C. The electrochemical cell used was the same as that used for Ni–Cu deposition. A cathodic potential of −0.75 V was applied to yield a total passed charge of 50 mC/cm^2. SEM and XPS were used to examine the prepared electrodes. The crystal structure was explored using a glancing angle X-ray diffractometer (GAXRD, Rigaku D/MAX 2500), which is more surface sensitive as compared to a tradition XRD, since the thin deposit had a weak crystallinity. The amount of Co deposited on the substrates was quantified using an atomic absorption spectrometer (AAS, SOLAAR M6); in these analyses, the deposits were totally dissolved in 0.1 M HNO_3 solution for the measurements. The loading mass of $Co(OH)_2$ was found to be approximately 25 μg/cm^2.

The electrochemical properties of the prepared electrodes with various substrates were studied using cyclic voltammetry (CV) and chronopotentiometry (CP) in 1 M KOH solution at 25 °C. The CV potential was scanned in a range of −0.2∼0.45 V with sweep rates ranging from 5 to 200 mV/s. CP was performed at a constant current density of ±0.5 mA/cm^2 to characterize the charge–discharge performance and cyclic stability of the electrodes.

3. Results and discussion

A cyclic voltammogram of the Ni foil in the Ni(II) and Cu(II) mixed solution was recorded (see ESI Fig. SI1†). When the electrode was cathodically polarized from its open-circuit potential (∼0.1 V), the onset of Cu reduction current was approximately at 0 V. Since Cu(II) has a mass transfer limitation due to its low concentration, the deposition current did not significantly vary with potential until −0.7 V, at which point Ni(II) reduction began. The distinct anodic peaks, at 0.1 V and 0.2 V, can be attributed to the stripping of the outmost pure Cu (last deposited during the reverse scan) and the selective dissolution of Cu from the underlying Ni–Cu layer, respectively. To further understand the reaction mechanism, XPS was used to examine the chemistry of the deposits. Fig. 1 (a) shows the Ni $2p_{3/2}$ and Cu $2p_{3/2}$ spectra taken from the film deposited at

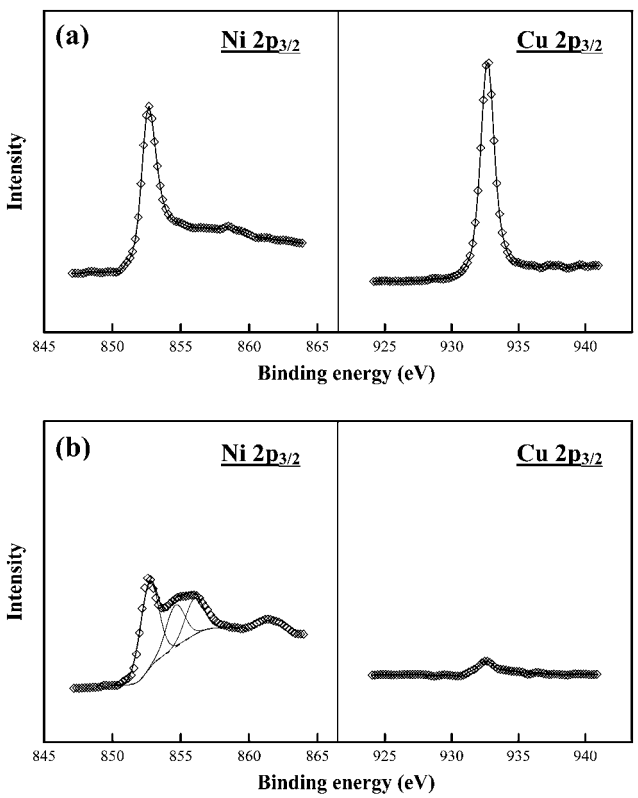

Fig. 1 XPS Ni $2p_{3/2}$ and Cu $2p_{3/2}$ spectra taken from (a) the −0.75 V as-deposited film, and (b) the +0.2 V etched film. The electrodeposition and selective dissolution were performed in a 1 M $NiSO_4$, 0.01 M $CuSO_4$, and 0.5 M H_3BO_3 mixed solution.

−0.75 V. The binding energy peaks located at 852.7 eV and 932.7 eV correspond to the zero valences of Ni and Cu, respectively.[33,34] Moreover, the Ni to Cu atomic ratio was found to be 40:60, confirming the co-deposition of a metallic form of alloy at this applied potential. The sample was then etched at 0.2 V and again analyzed with XPS; the obtained spectra are shown in Fig. 1 (b). As demonstrated, the Ni peak is much broader than that in Fig. 1 (a) and can be deconvoluted into three components. Besides the Ni(0) signal, the constituents at 854.6 eV and 856.0 eV were associated with NiO and Ni_2O_3, respectively.[33,35] The Cu peak intensity greatly decreased after etching. The results clearly confirm that due to the formation of a surface oxide layer in the sulfate solution, Ni was passivated and remained on the electrode while Cu was selectively removed under the anodic applied potential. These analytical data explain why the integrated anodic charge in Fig. 1 is only about one-third of the cathodic one. Since the co-deposition of Ni–Cu and the selective dissolution of Cu can be performed in the same solution by simply switching the potential, we used this facile technique to fabricate high-surface-area Ni substrates for use in supercapacitors.

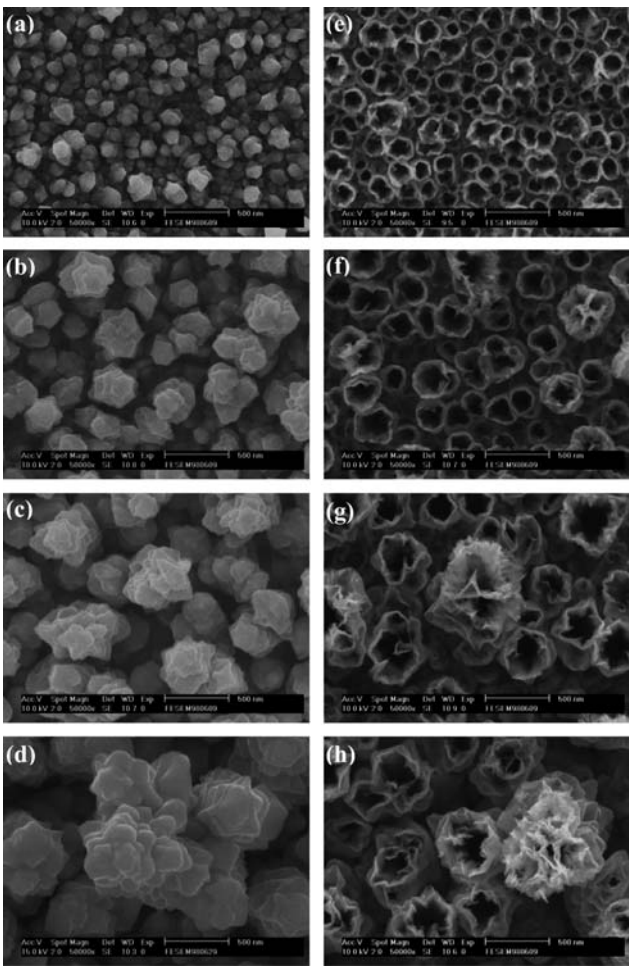

Fig. 2 (a)–(d) SEM micrographs of Ni–Cu films with deposition charges of 1, 2, 3, and 4 C/cm^2, respectively. (e)–(h) Porous structures developed from (a)–(d), respectively, after being selectively etched.

Fig. 2 (a)–(d) show the SEM micrographs of the Ni–Cu films deposited at −0.75 V with total cathodic charges of 1, 2, 3, and 4 C/cm^2, respectively. With increasing deposition charge, new grains seemed to form on previous ones (*i.e.* progressive nucleation), growing into a protruding structure. While the grains did not significantly change in size (∼100 nm in diameter), they tended to overlap and aggregate into clusters while the passed charge was accumulated. EDS analyses confirmed that the Ni/Cu atomic ratios of the samples in Fig. 2 (a)–(d) were all close to 40/60, which is consistent with the XPS data, revealing a uniform distribution of the chemical composition with depth. Fig. 2 (e)–(h) show the porous structures developed from the films in Fig. 2 (a)–(d), respectively, after being etched at 0.2 V. The results given in Fig. 1 and 2 suggest that the central part of each grain was a Cu-rich domain that was preferentially dissolved when the anodic potential was applied, creating the hollow Ni nano-structures. Chemical segregation within deposited Ni–Cu grains was also observed in previous Auger electron mapping and TEM studies.[27,28] For the Ni-1C sample (Fig. 2 (e)), hollow tubes with a diameter of around 100 nm and a pore density of approximately 10^{13}/m^2 were observed. The morphologies gradually became petal-like structures (from Ni-2C to Ni-4C), because the clustering of the Ni–Cu grains led to formation of connected pores upon etching. The average pore size in Fig. 2 (h) increased to approximately 200 nm with a decrease in the pore density. It was found from the SEM cross-section observation that the thickness of the porous layer increased from ∼1 to ∼4 μm with increasing the deposition charge from 1 to 4 C/cm^2. The residual Cu in the porous electrodes, inspected using EDS, was less than 3 at.% regardless of film thickness, confirming that most of the Cu was extracted from the deposits. Therefore, we have developed an efficient electrochemical protocol for constructing Ni nano-structured layers with various porosities and thicknesses. The feature size of the obtained architectures is much smaller than those of the existing Ni foam and stainless steel mesh substrates used for pseudoapacitors;[23–25] thus, more improvements in the performance of an electroactive material are expected.

To achieve an entirely electrochemical procedure for fabricating a nano-structured capacitor electrode, direct electrodeposition of $Co(OH)_2$ on the prepared Ni substrates was attempted. The linear sweep voltammogram (LSV) of a porous Ni electrode was recorded in 0.1 M $Co(CH_3COO)_2$ aqueous solution with a pH of 7.4 (see ESI Fig. SI2†). When the electrode was polarized from its open circuit potential (∼−0.05 V), a cathodic current began to increase at approximately −0.7 V, which is close to the theoretical hydrogen evolution potential (*i.e.* −0.678 V *vs.* SCE) under the given pH value. After the LSV measurement, the electrode was subjected to GAXRD analysis; the obtained diffraction pattern is shown in Fig. 3 (a). Besides the two strong peaks associated with the Ni substrate, the peaks located at 19.0° and 37.8° were identified to be the (001) and (101) diffraction signals of $Co(OH)_2$ with a hexagonal structure (JCPDS No. 73-6993), verifying an electrodeposition of the hydroxide. The broad diffraction peaks with low intensity suggest that the deposited $Co(OH)_2$ could be nano-crystalline. Fig. 3 (b) and (c) show the Co $2p_{3/2}$ and O 1s XPS spectra of the deposit. As shown, the Co spectrum is composed of two constituents; besides the major peak of $Co(OH)_2$ located at the

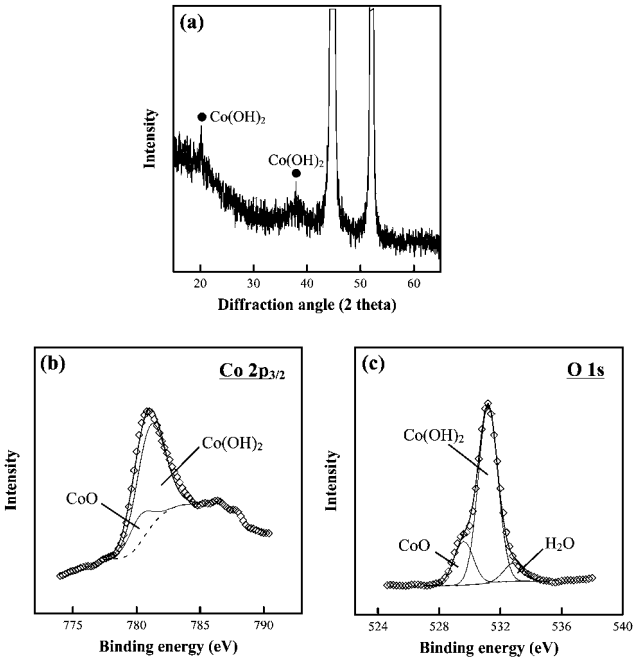

Fig. 3 (a) GAXRD pattern, (b) XPS Co $2p_{3/2}$ spectrum, and (c) XPS O 1s spectrum taken from the electrode subjected to the measurement in Fig. 4.

binding energy of 781.1 eV, the CoO compound contributed a minor signal at 780.2 eV.[33] The curve fitting results of the O 1s spectrum supports that $Co(OH)_2$ (531.2 eV) was the predominant species within the deposit. Two smaller shoulders, attributed to CoO (529.6 eV) and structural water (532.9 eV), were also found.[36,37] The amount of Co deposited was quantified with an AAS; the analytical data revealed that the mole number of Co was always close to half the mole number of passed electrons (regardless of the deposition charge and the substrate porosity), suggesting a two-charge transfer reaction during the electrodeposition. According to the deposition potential, the obtained species, and the charge transfer number, the mechanism of the observed deposition reaction can be essentially described as follows:

$$H_2O + 2e^- \rightarrow H_2 + 2OH^- \quad (1)$$

$$Co^{2+} + 2OH^- \rightarrow Co(OH)_2 \quad (2)$$

Since a rapid gas evolution occurred at a more negative applied potential, leading to the non-uniformity of the deposited layer, a potential of −0.75 V was adopted for the subsequent potentiostatic depositions.

Fig. 4 (a) and (b) show the morphologies of the prepared $Co(OH)_2$ electrodes with flat Ni and Ni-3C substrates, respectively. On the flat substrate, relatively massive hydroxide ribbons were observed above a granular but compact lower layer. On the other hand, the nano-porous Ni provided a larger area for dispersing the deposit. As shown, silk-like $Co(OH)_2$ with a width of just a few nano-meters was uniformly distributed on the nano-sized Ni petals, even inside the pores. This proves that a nano-structured $Co(OH)_2$ electrode was successfully constructed.

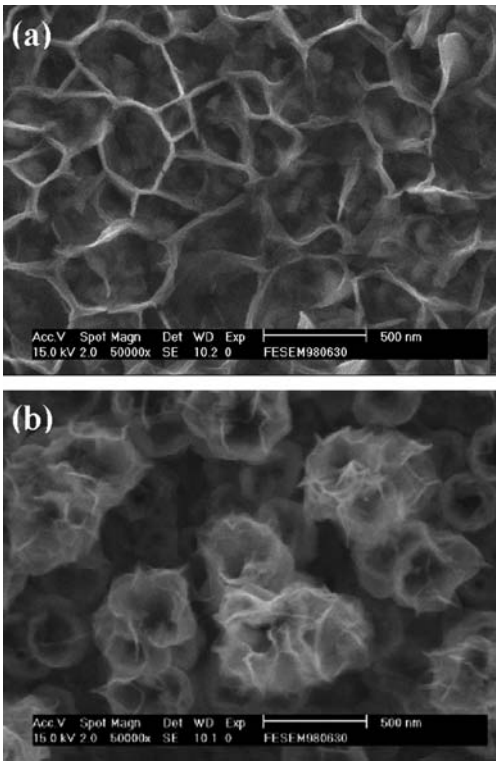

Fig. 4 SEM micrographs of the prepared $Co(OH)_2$ electrodes with (a) a flat Ni substrate and (b) the nano-porous Ni-3C substrate.

The pseudocapacitive characteristics of this electrode were then systematically evaluated, as discussed in the following sections.

Fig. 5 (a) shows the cyclic voltammograms of $Co(OH)_2$ electrodes with Ni-1C, Ni-2C, Ni-3C, and Ni-4C substrates recorded in 1 M KOH solution. Within the potential scanning range, two symmetric anodic/cathodic pairs superimposed on a broad redox background were recognized, indicating that reversible pseudocapacitive reactions of $Co(OH)_2$ were involved. According to the literature,[11,25] the observed two redox couples can be expressed as:

$$Co(OH)_2 + OH^- \leftrightarrow CoOOH + H_2O + e^- \quad (3)$$

$$CoOOH + OH^- \leftrightarrow CoO_2 + H_2O + e^- \quad (4)$$

It should be noted that in Fig. 5 (a), the CV curve enclosed area, which corresponds to the energy storage capability, increases with increasing thickness of the nano-porous Ni layers. The Ni substrate did not materially expose to the electrolyte and contribute to a noticeable redox signal (see ESI Fig. SI3†). The specific capacitance (C) of $Co(OH)_2$ on various substrates can be quantitatively evaluated using the following equation:

$$C = Q_m/\Delta V \quad (5)$$

where Q_m is the specific voltammetric charge (based on the mass of $Co(OH)_2$) integrated from both the positive and negative CV sweeps, and ΔV is the potential scanning extent (*i.e.* 0.65 V × 2). The calculated capacitances of $Co(OH)_2$ deposited on the Ni-1C, Ni-2C, Ni-3C, and Ni-4C electrodes were 1250, 2100, 2650, and 2800 F/g, respectively. In contrast, the counterpart $Co(OH)_2$ on

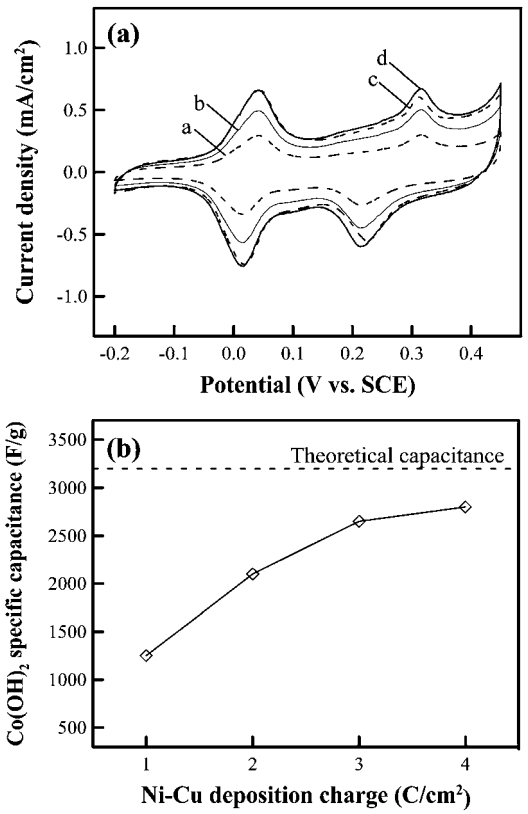

Fig. 5 (a) Cyclic voltammograms of $Co(OH)_2$ electrodes with the Ni-1C (curve a), Ni-2C (curve b), Ni-3C (curve c), and Ni-4C (curve d) substrates recorded in 1 M KOH solution with a potential sweep rate of 5 mV/s. (b) The calculated specific capacitances of $Co(OH)_2$ on the various substrates.

a flat substrate showed a capacitance of only 550 F/g, which is close to those typically reported in the literature.[10,23,38,39] The high surface area of the nano-structured electrode significantly extended the electro-active sites for pseudocapacitive reactions. Moreover, the high-porosity architecture enhanced the electrolyte accessibility and thereby led to superior electrode reactivity. As a result, the nano-structured $Co(OH)_2$ electrodes exhibited much better energy storage performance as compared to that of the traditional version of the electrode. The exceptional capacitance of 2800 F/g is the highest value achieved so far for the $Co(OH)_2$ electrode, except for that obtained by Cao *et al.*[11] using a co-precipitation preparation process, which was more complicated than electrodeposition. They prepared a $Co(OH)_2$/zeolite nano-composite with a measured capacitance of 1492 F/g and speculated that the $Co(OH)_2$ alone (assuming that the zeolite was inert) may possess a specific capacitance of around 3000 F/g. According to Eqn (3) and (4), the theoretical specific capacitance of $Co(OH)_2$ over a potential range of 0.65 V is 3195 F/g. Fig. 5 (b) indicates that the nano-structured $Co(OH)_2$ approaches complete utilization with increasing thickness of the porous Ni layers. More specifically, an utilization of as high as 88% can be achieved on the Ni-4C substrate due to the high dispersion of $Co(OH)_2$; this ratio is over five times higher than that (~17%) of the conventional $Co(OH)_2$ counterpart. High utilization also implies a possibility of reducing the amount of active material used (and thus the cost of the electrode), preserving natural resources.

Fig. 6 (a) shows the CV curves of nano-structured $Co(OH)_2$ with the Ni-4C substrate measured at various potential sweep rates. The mirror-image characteristics (with symmetric anodic and cathodic peaks) can be maintained even at a high rate of 200 mV/s. Moreover, the response current of the electrode increased almost linearly with the potential sweep rate. This reveals the excellent kinetic performance and reversibility of the nano-structured electrode. Fig. 6 (b) summarizes the capacitance retained ratios as a function of CV scan rate of the electrodes prepared in this study. When the potential scan rate was increased from 5 to 200 mV/s, the $Co(OH)_2$ electrodes with the flat Ni, Ni-1C, Ni-2C, Ni-3C, and Ni-4C substrates reserved 67, 84, 89, 93, and 96% of their initial capacitances, respectively. The superior high-rate performance of the nano-structured electrode can be attributed to three major factors: (i) the high porosity increases OH^- transport, promoting the ionic conduction within the electrode, (ii) the greatly dispersed $Co(OH)_2$ shortens the electron traveling distance, improving the electronic conduction, and (iii) the high contact area between the substrate and the electro-active material minimizes the interface resistance, facilitating charge transfer reactions. It should be noted that the optimum $Co(OH)_2$ electrode (with the Ni-4C substrate) showed a capacitance of as high as 2700 F/g at 200 mV/s; this high-rate

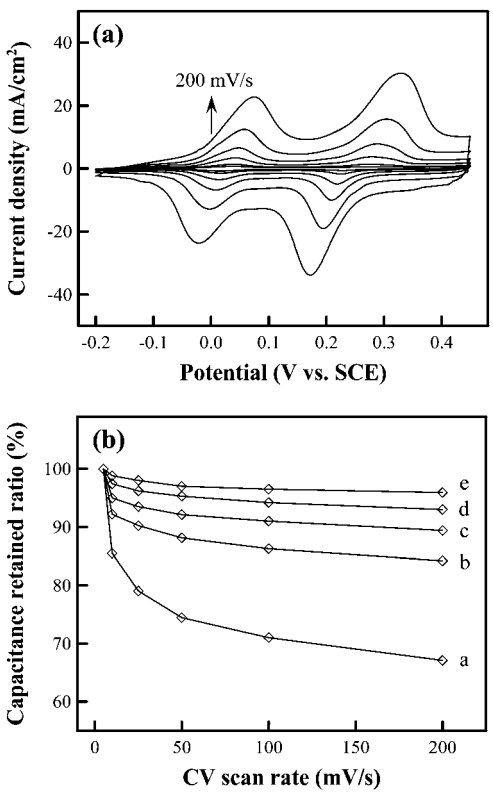

Fig. 6 (a) Cyclic voltammograms of the nano-structured $Co(OH)_2$ electrode with the Ni-4C substrate measured at various potential sweep rates, ranging from 5 to 200 mV/s. (b) Capacitance retained ratios as a function of the CV sweep rate of $Co(OH)_2$ electrodes with flat Ni (curve a), Ni-1C (curve b), Ni-2C (curve c), Ni-3C (curve d), and Ni-4C (curve e) substrates.

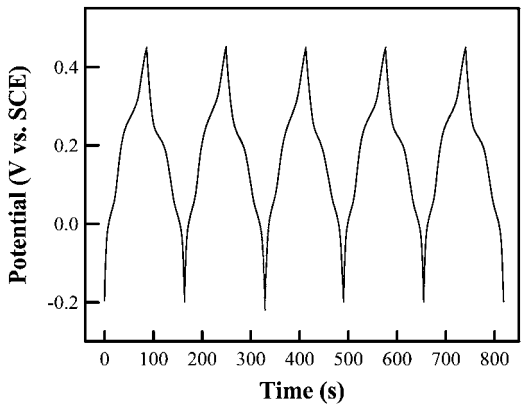

Fig. 7 Chronopotentiogram of the nano-structured $Co(OH)_2$ electrode with the Ni-4C substrate. The measurement was performed with a constant current density of ± 0.5 mA/cm^2 in 1 M KOH solution.

capability, to the best of our knowledge, outperforms any existing $Co(OH)_2$ electrode reported in the literature.[8,10,12,23,25] This result indicates the potential of using the proposed strategy to construct supercapacitor nano-structured electrodes, since their high-power performance is of a crucial concern.

The galvanostatic charge–discharge performance of the nano-structured electrodes was further characterized by CP. Fig. 7 shows a typical chronopotentiogram, including five charge–discharge cycles, of the $Co(OH)_2$ electrode with the Ni-4C substrate. The symmetric and quasi-linear characteristics of the anodic and cathodic branches indicate the capacitive behavior of the electrode. As shown, slight potential plateaus were found at 0.05 V and 0.25 V, which corresponded to the two redox pairs observed in the CV curve, respectively. The specific capacitance of $Co(OH)_2$ can be also measured using CP according to:

$$C = I\,\Delta t/\Delta E\,w \qquad (6)$$

where I is the applied current (0.5 mA), ΔE is the potential range (0.65 V $\times$ 2), Δt is the time of a charge–discharge cycle, and w is the mass of $Co(OH)_2$. The calculated capacitance was as high as 2750 F/g, which was very close to that estimated from CV, again confirming the extraordinary charge storage capacity. The electrochemical stability of the electrodes was evaluated by repeating the CP cycling. It was found that the $Co(OH)_2$ deposited on a flat substrate suffered a 25% capacitance decay after 500 charge–discharge cycles. AAS analytical data revealed that only 75% of the initial $Co(OH)_2$ remained after the cycling, indicating that the capacitance fading was mainly attributed to the loss of the active material. In contrast, the nanostructured $Co(OH)_2$ electrode (with the Ni-4C substrate) did not show capacitance deterioration even after 2000 cycles ($\sim$2850 F/g, see ESI Fig. SI4†); according to AAS analyses, more than 96% of the $Co(OH)_2$ remained on the electrode. The slightly increased capacitance probably resulted from the incorporation of Ni hydroxide/oxide into $Co(OH)_2$ upon prolonged cycling. Although the detailed mechanism should be further investigated, the excellent cyclic stability of the nano-structured electrode may be associated with the superior reaction homogeneity, due to improved electronic and ionic conduction, that benefits electrode reversibility. Moreover, the Ni nano-architecture could act as a hard template for suppressing the re-agglomeration of $Co(OH)_2$ and help confine the electro-active material, preventing it from detachment and/or dissolution upon cycling.

4. Conclusion

An efficient procedure for constructing nano-structured $Co(OH)_2$ supercapacitor electrodes was proposed. In general, the process can be implemented on any conductive surface using an entirely electrochemical protocol, which is inexpensive and easily manipulated. The created nano-structures are self-supported and binder-less. Due to its unique architecture, the prepared $Co(OH)_2$ electrode provides a large surface area for electrochemical reactions, high porosity for electrolyte accessibility, and great dispersion of the active material for shortening the electron and ion traveling distances. As a result, the electrode exhibits an exceptional pseudocapacitance of as high as 2800 F/g and an outstanding high-rate redox capability. The nano-porous substrate also preserves the active material cyclic stability. The proposed method of fabricating nano-structured electrodes is expected to be applicable to loading other active materials to improve their sensing, catalytic, and energy-conversion/storage performances.

Acknowledgements

The financial support of this work by the National Science Council of the Republic of China under grant NSC 98-ET-E-006-009-ET is gratefully appreciated.

References

1 *Electrochemical Supercapacitors*, ed. B. E. Conway, Kluwer-Plenum, New York, 1999.
2 P. Simon and Y. Gogotsi, *Nat. Mater.*, 2008, **7**, 845.
3 K. W. Nam, M. G. Kim and K. B. Kim, *J. Phys. Chem. C*, 2007, **111**, 749.
4 J. K. Chang, M. T. Lee and W. T. Tsai, *J. Power Sources*, 2007, **166**, 590.
5 J. P. Zheng, P. J. Cygan and T. R. Jow, *J. Electrochem. Soc.*, 1995, **142**, 2699.
6 W. Sugimoto, H. Iwata, Y. Yasunaga, Y. Murakami and Y. Takasu, *Angew. Chem., Int. Ed.*, 2003, **42**, 4092.
7 C. C. Hu, K. H. Chang, M. C. Lin and Y. T. Wu, *Nano Lett.*, 2006, **6**, 2690.
8 V. Gupta, T. Kusahara, H. Toyama, S. Gupta and N. Miura, *Electrochem. Commun.*, 2007, **9**, 2315.
9 H. J. Ahn, W. B. Kim and T. Y. Seong, *Electrochem. Commun.*, 2008, **10**, 1284.
10 P. K. Nayak and N. Munichandraiah, *J. Electrochem. Soc.*, 2008, **155**, A855.
11 L. Cao, F. Xu, Y. Y. Liang and H. L. Li, *Adv. Mater.*, 2004, **16**, 1853.
12 W. J. Zhou, J. Zhang, T. Xue, D. D. Zhao and H. L. Li, *J. Mater. Chem.*, 2008, **18**, 905.
13 Z. L. Wang, *Adv. Mater.*, 2003, **15**, 1497.
14 R. H. Baughman, A. A. Zakhidov and W. A. de Heer, *Science*, 2002, **297**, 787.
15 A. S. Aricò, P. Bruce, B. Scrosati, J. M. Tarascon and W. van Schalkwijk, *Nat. Mater.*, 2005, **4**, 366.
16 D. Choi, G. E. Blomgren and P. N. Kumta, *Adv. Mater.*, 2006, **18**, 1178.
17 J. K. Chang, C. H. Huang, W. T. Tsai, M. J. Deng and I. W. Sun, *J. Power Sources*, 2008, **179**, 435.
18 Y. Wang, K. Takahashi, K. H. Lee and G. Z. Cao, *Adv. Funct. Mater.*, 2006, **16**, 1133.
19 R. Liu and S. B. Lee, *J. Am. Chem. Soc.*, 2008, **130**, 2942.

20 A. E. Fischer, K. A. Pettigrew, D. R. Rolison, R. M. Stroud and J. W. Long, *Nano Lett.*, 2007, **7**, 281.
21 S. L. Chou, J. Z. Wang, S. Y. Chew, H. K. Liu and S. X. Dou, *Electrochem. Commun.*, 2008, **10**, 1724.
22 K. W. Nam, C. W. Lee, X. Q. Yang, B. W. Cho, W. S. Yoon and K. B. Kim, *J. Power Sources*, 2009, **188**, 323.
23 S. L. Chou, J. Z. Wang, H. K. Liu and S. X. Dou, *J. Electrochem. Soc.*, 2008, **155**, A926.
24 G. W. Yang, C. L. Xu and H. L. Li, *Chem. Commun.*, 2008, 6537.
25 W. J. Zhou, M. W. Xu, D. D. Zhao, C. L. Xu and H. L. Li, *Microporous Mesoporous Mater.*, 2009, **117**, 55.
26 L. Sun, C. L. Chien and P. C. Searson, *Chem. Mater.*, 2004, **16**, 3125.
27 J. K. Chang, S. H. Hsu, I. W. Sun and W. T. Tsai, *J. Phys. Chem. C*, 2008, **112**, 1371.
28 Z. Liu, D. Elbert, C. L. Chien and P. C. Searson, *Nano Lett.*, 2008, **8**, 2166.
29 J. K. Chang, S. H. Hsu, W. T. Tsai and I. W. Sun, *J. Power Sources*, 2008, **177**, 676.
30 M. J. Deng, F. L. Huang, I. W. Sun, W. T. Tsai and J. K. Chang, *Nanotechnology*, 2009, **20**, 175602.
31 G. S. Attard, P. N. Bartlett, N. R. B. Coleman, J. M. Elliott, J. R. Owen and J. H. Wang, *Science*, 1997, **278**, 838.
32 P. A. Nelson, J. M. Elliott, G. S. Attard and J. R. Owen, *Chem. Mater.*, 2002, **14**, 524.
33 T. L. Barr, *J. Phys. Chem.*, 1978, **82**, 1801.
34 P. Marcus and M. E. Bussell, *Appl. Surf. Sci.*, 1992, **59**, 7.
35 *Handbook of X-ray Photoelectron Spectroscopy*, ed. J. Chastain and R. C. King Jr., Physical Electronics Inc., Minnesota, 1995.
36 *Practical Surface Analysis: Auger and X-Ray Photoelectron Spectroscopy*, ed. D. Briggs and M. P. Seah, John Wiley & Sons, New York, 1996.
37 N. S. McIntyre and M. G. Cook, *Anal. Chem.*, 1975, **47**, 2208.
38 C. Yuan, X. Zhang, B. Gao and J. Li, *Mater. Chem. Phys.*, 2007, **101**, 148.
39 Z. Hu, L. Mo, X. Feng, J. Shi, Y. Wang and Y. Xie, *Mater. Chem. Phys.*, 2009, **114**, 53.